

Frustration-induced valence bond crystal and its melting in Mo_3Sb_7

T. Koyama,¹ H. Yamashita,¹ Y. Takahashi,¹ T. Kohara,¹ I. Watanabe,² Y. Tabata,³ and H. Nakamura³

¹*Graduate School of Material Science, University of Hyogo, Kamigori, Ako-gun, Hyogo 678-1297, Japan*

²*Advanced Meson Science Laboratory, RIKEN Nishina Center, Wako 351-0198, Japan*

³*Department of Materials Science and Engineering, Kyoto University, Kyoto 606-8501, Japan*

(Dated: February 2, 2022)

$^{121/123}\text{Sb}$ nuclear quadrupole resonance and muon spin relaxation experiments of Mo_3Sb_7 revealed symmetry breakdown to a nonmagnetic state below the transition recently found at $T_S \simeq 50$ K. The transition is characterized by a distinct lattice dynamics suggested from narrowing of nuclear fields. We point out that the Mo sublattice is a unique three-dimensional frustrated lattice where nearest-neighbor and next-nearest-neighbor antiferromagnetic interactions compete, and propose that tetragonal distortion to release the frustration stabilizes long-range order of spin-singlet dimers, i.e., valence bond crystal, which is thermally excited to the dynamic state with cubic symmetry.

PACS numbers: 71.20.Be, 76.60.-k, 76.75.+i

Exotic phenomena induced by the geometric frustration have attracted great interest, and trial to find novel phases in various types of frustrated lattices has been going on [1]. In the case of three-dimensional (3D) pyrochlore lattice, the symmetry breakdown to spin-Peierls-like states or to the valence bond crystal with the quenched spin degrees of freedom [2, 3] is one of the options to release the frustration; a typical example is found in the case of MgTi_2O_4 [4]. On the other hand, in the field of correlated-electron superconductivity (SC), another phase transition prior to SC, such as the antiferromagnetic (AF) or hidden order [5], attracts interest, because the particular electronic states may be a key to understand the unconventional SC.

A metallic compound Mo_3Sb_7 , with the cubic Ir_3Ge_7 type structure (space group $Im\bar{3}m$), is a superconductor with a critical temperature $T_c \simeq 2.3$ K [6]. As seen in the inset of Fig. 1(a), the Mo sublattice (12e) is the 3D network of Mo-Mo dumbbells formed by nearest neighbors (NN). Next-nearest-neighbor (NNN) bonds form an octahedral cage at the body-centered position. The sufficiently short NN distance (3.0 Å) comparing with the NNN distance (4.6 Å) makes us anticipate easy dimerization between NN pairs. Recently, Candolfi *et al.* [7] regarded Mo_3Sb_7 as an itinerant electron system and suggested coexistence of SC and spin fluctuations, which is a rare example in d electron metals. A broad maximum in the temperature (T) dependence of the susceptibility (χ) with relatively large magnitude, a large electronic specific heat coefficient, a T^2 dependence of low- T electrical resistivity, the Kadowaki-Wood relation between the specific heat and the resistivity, *etc.* point to the presence of strong electron correlation. Band structure calculations for cubic Mo_3Sb_7 [8, 9], showing appreciable contribution of Mo-4d orbitals to the density of states near the Fermi level, are in agreement with these observations. Although no phase transition other than that at T_c was known in [7], Tran *et al.* [10] reported recently the presence of another phase transition at $T^* \simeq 50$ K (in this article, referred to as T_S), and proposed spin gap formation with the magnitude of 120 K associated with Mo-Mo

dimerization. Here the Mo^{5+} state with spin $S = 1/2$ was presumed implicitly. In fact at sufficiently high T , χ shows a $S = 1/2$ Curie-Weiss behavior with a large negative Weiss constant, suggesting strong AF interaction among active Mo spins. Thus the Mo electronic state is of interest as the system with both itinerant and localized characters. Furthermore Mo_3Sb_7 is now recognized as a new material with another phase transition prior to SC. As for SC, the pairing mechanism is still controversial. Although most studies point to a BCS-type conventional SC [6, 9, 11, 12], unconventional pairing has also been discussed [12, 13]. In [10], it was argued that the Fermi surface nesting leads to SC.

In this article, to manifest microscopic and dynamic aspects of the magnetism in Mo_3Sb_7 , particularly to identify the phase between T_c and T_S , we present $^{121/123}\text{Sb}$ nuclear quadrupole resonance (NQR) and muon spin relaxation (μSR) results together with low- T x-ray diffraction (XRD) data. We discuss possible frustration in the Mo sublattice by assuming AF NN and NNN interactions, and propose new exotic states realized due to the competition between NN and NNN interactions.

Polycrystalline Mo_3Sb_7 specimen were prepared via reaction between liquid Sb and solid Mo. NQR spin-echo measurements were carried out using a conventional phase-coherent-type pulse spectrometer at 1.4–200 K. Zero-field (ZF) μSR measurements were made at RIKEN-RAL Muon Facility at the Rutherford-Appleton Laboratory in the UK using a pulsed positive surface muon beam at 5–250 K. Low- T powder XRD was measured using a conventional diffractometer (MacScience MXP) with $\text{Cu } K\alpha$ radiation.

Figure 1(a) shows the $^{121/123}\text{Sb}$ NQR spectrum of Mo_3Sb_7 at 200 K. Antimony has two isotopes ^{121}Sb (nuclear spin $I = 5/2$) and ^{123}Sb ($I = 7/2$), which yield two and three quadrupole transition lines, respectively, when the electric field gradient (EFG) is axially symmetric. In cubic Mo_3Sb_7 , there are two nonequivalent Sb positions with nonaxial and axial symmetries (12d and 16f, respectively). We have found only five lines at 200 K corresponding to either site. This is probably because

the nuclear spin relaxation rate at the unobserved site is enhanced due to fast fluctuations of active Mo electron spins. The frequency intervals between neighboring lines of $^{121/123}\text{Sb}$ are approximately equal, indicating nearly axial EFG at the observed site. $^{121/123}\text{Sb}$ quadrupole frequencies are $^{121/123}\nu_Q \simeq 47.7/27.2$ MHz at 200 K.

The T dependence of the ^{121}Sb - $2\nu_Q$ line (transitions of $|\pm 3/2\rangle \leftrightarrow |\pm 5/2\rangle$) is shown in Fig. 1(b). The line is shifted to the high frequency side and gradually broadened with approaching T_S . At $\sim T_S$, the line loses intensity and disappears due to highly enhanced spin-echo decay rate $1/T_2$ (see the inset of Fig. 2). Below 20 K the signal reappears with complicated structures (see a part of the data at 10 K in Fig. 1(b)). Actually ZF nuclear resonance signal was continuously observed in almost the whole frequency range below 110 MHz with a number of peaks. This indicates clearly symmetry breakdown below T_S . The origin is either appearance of the internal field (due to magnetic order), separation of crystallographic Sb sites (due to structural deformation) or both. Unfortunately, the spectrum at low T is too complicated and unresolved to conclude this issue because of line split together with broadening, as well as the possible emergence of the signal from another Sb site. An early ^{121}Sb Mössbauer study is not articulate either [14]. Hence, to determine the magnetic ground state, we employ another microscopic probe, μSR , which is sensitive to the appearance of the internal field; the result will be shown below.

The nuclear spin-lattice relaxation rate $1/T_1$ was measured for both ^{121}Sb - and ^{123}Sb - $2\nu_Q$ transitions. Nuclear magnetization recovery was fitted well using the multi-exponential function with a single parameter expected for the case of axial EFG [15, 16]. The ratio of relaxation rates for the different isotopes was estimated to be $^{123}T_1/^{121}T_1 \simeq 3.5$ at $T > T_S$, which is close to the squared gyromagnetic ratios $^{121}\gamma_n^2/^{123}\gamma_n^2 \simeq 3.4$. This confirms that the relaxation process is not by fluctuations of EFG but by those of the internal magnetic field at least above T_S . $1/T_1$ was measured at the peak position of the ^{121}Sb - $2\nu_Q$ line and plotted in the form of $1/(T_1T)$ vs. T in Fig. 2. The divergent behavior was observed at $\sim T_S$, although reliable values of $1/T_1$ could not be obtained near T_S due to poor signal-to-noise ratio [17]. In fact, the transition at T_S is characterized by the stronger T dependence of $1/T_2$ (the inset of Fig. 2); $1/T_2 \sim 10\text{--}10^3(1/T_1)$. Below T_S , $1/(T_1T)$ decreases rapidly with decreasing T , being consistent with the possible existence of spin gap [10], but turns to show a $T_1T = \text{constant}$ Korringa behavior below ~ 10 K, indicating the presence of residual density of states at the Fermi level, which is related with the residual χ at low T . $1/T_1$ is enhanced just below T_c . Such an enhancement is known as a coherence peak and usually observed for the conventional BCS superconductor with an isotropic gap [18].

Now we shift to μSR results. Typical examples of ZF- μSR spectra are shown in the inset of Fig. 3. Even at the lowest T (5 K), no straightforward evidence of

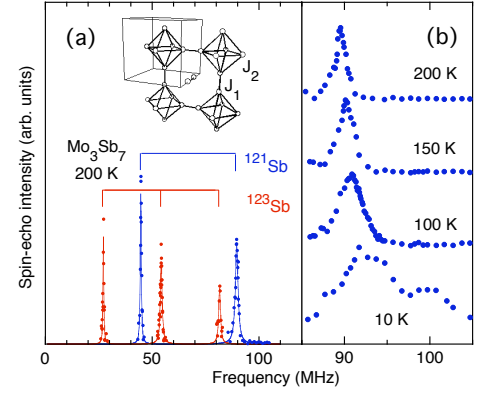


FIG. 1: (color online). (a) $^{121/123}\text{Sb}$ NQR spectrum of Mo_3Sb_7 at 200 K. Inset shows the Mo sublattice. (b) Temperature variation of ^{121}Sb - $2\nu_Q$ line.

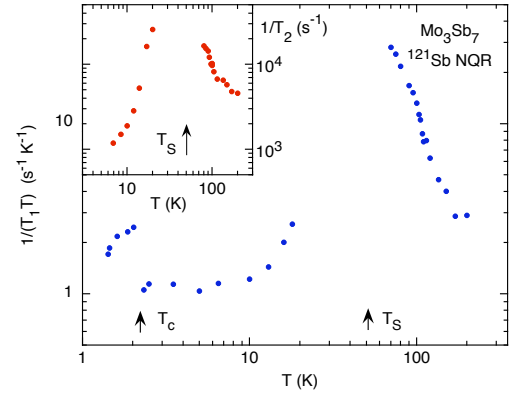


FIG. 2: (color online). Temperature dependence of ^{121}Sb - $1/(T_1T)$ for Mo_3Sb_7 . Inset shows the temperature dependence of $1/T_2$.

magnetic order such as muon spin precession was observed. At all T , the feature of relaxation is essentially the same and shows Gaussian-like depolarization. The commonly used damped Kubo-Toyabe (KT) function $P_\mu(t) = \exp(-\Lambda t) G_z^{\text{KT}}(\Delta, t)$ with $G_z^{\text{KT}}(\Delta, t) = \frac{1}{3} + \frac{2}{3}(1 - \Delta^2 t^2) \exp(-\frac{1}{2}\Delta^2 t^2)$ was fit to the data, where Δ/γ_μ is the width of the static field distribution (γ_μ the muon gyromagnetic ratio), and Λ is the damping rate associated with an additional relaxation process. As seen below, it is likely that the KT term is dominated by the nuclear dipolar field and the damping part reflects the Mo electronic system. Figure 3 shows the T dependence of Δ . First, let us see the T -independent part in the intermediate T range of $\sim 70\text{--}140$ K with $\Delta/\gamma_\mu \simeq 0.25$ G. This tiny field is most probably due to dipolar fields coming from randomly oriented nuclear spins. Above ~ 140 K, Δ is reduced markedly. As shown in Fig. 4, $\ln \Delta$ is in proportion to $1/T$ in the T range, suggesting a motional narrowing process caused by muon hopping among different sites, that is frequently observed at high T ; the activation energy is $E_a/k_B \simeq 910$ K. With decreasing T passing through T_S , Δ is enhanced strongly as seen in Fig. 3.

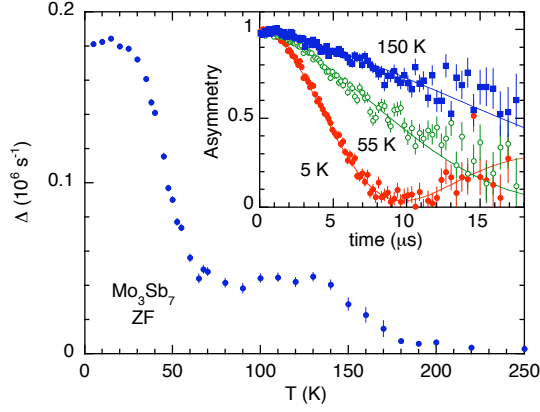


FIG. 3: (color online). Temperature dependence of the ZF Kubo-Toyabe relaxation rate Δ in Mo_3Sb_7 . Inset shows typical examples of ZF- μSR spectra (at 5, 55 and 150 K). Solid curves indicate the fit by the damped KT function.

This behavior is clearly related with the transition at T_S . The origin of the additional internal field below T_S is the most essential point in this experiment. The Gaussian-type random distribution with small $\Delta/\gamma_\mu \simeq 2.1$ G even at the lowest T is hardly attributed to the electron spin freezing but is reasonably explained as due to the change in nuclear dipolar field associated with the structural deformation mentioned below [19]. The T dependence of Δ at $\sim T_S$ is again explained as a thermal excitation process with activation energy of $E_a/k_B \simeq 120$ K. This implies that the T variation is dominated by a *dynamic* process, giving very fruitful information on the nature of the transition at T_S .

The T dependence of Λ is shown in the inset of Fig. 4. The decrease above ~ 150 K would be analytical artifact due to the evolution of the relaxation process associated with the dynamic muon hopping. Λ has a sharp peak at T_S and decreases rapidly below T_S . This behavior is qualitatively same as that of NQR- $1/T_1$, and reflects the phase transition in the Mo electronic system. The quantitative difference in NQR- $1/T_1$ and μSR - Λ is most probably due to the difference in the coupling mechanism; the interaction between Sb nuclei and Mo electrons is probably dominated by the direct hyperfine coupling, while fields from Mo electrons to the muon site is by the dipolar mechanism. Different time windows of the measurements would also be appreciable. Furthermore, the muon stopping site may be a high symmetric position, say the center of the Mo cage, where the fields from Mo electron spins would mostly be canceled.

The μSR result points to the nonmagnetic ground state. This is in accordance with the spin-singlet dimerization suggested in [10]. To get information on the lattice symmetry below T_S , we made conventional XRD analyses at low T and found appreciable difference in the patterns below and above T_S . To see the change efficiently, we particularly show 600 diffraction peaks at 70 and 15 K in Fig. 5(a) [20]. As seen in the figure, a high- T

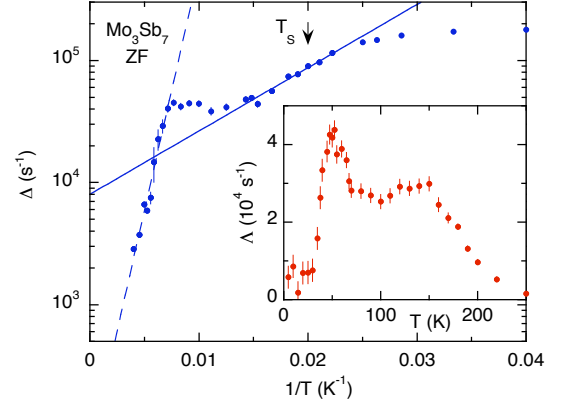


FIG. 4: (color online). ZF Kubo-Toyabe relaxation rate Δ in Mo_3Sb_7 plotted against $1/T$. Activation energies for two different thermal excitation processes are estimated to be 120 and 910 K from the solid and broken lines, respectively. Inset shows the temperature dependence of the relaxation rate Λ .

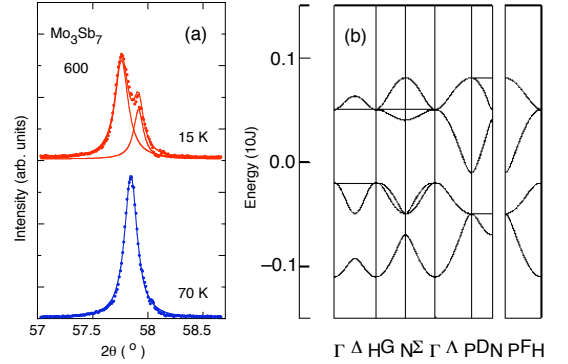


FIG. 5: (color online). (a) X-ray 600 peak of Mo_3Sb_7 at 70 K and its split pattern at 15 K [20]. The contribution of $K\alpha_2$ radiation is subtracted by profile fitting. (b) Dispersion curves of the exchange integral $J(q)$ of the Mo sublattice assuming negative J_1 and J_2 . $J_1 = -0.05$ and $J_2 = 0.3J_1$ were used arbitrarily.

singlet splits into double peaks with the intensity ratio of $\sim 2 : 1$ by crossing T_S , suggesting structural deformation from cubic to tetragonal (space group $I4/mmm$) as the simplest possibility; the estimated lattice parameter a is larger than c by $\sim 0.2\%$ at 15 K.

Although Mo_3Sb_7 is a metallic magnet, here we focus on the local nature of the Mo electron. Taking a glance at the Mo sublattice, if the NN interaction J_1 is dominant, no substantial symmetry breakdown is necessary to form dimers but isotropic shrinkage is sufficient. Therefore in discussing the mechanism of the transition, the low- T lattice symmetry is essential and NNN interaction J_2 should be taken into account. Note that positive (ferromagnetic) J_2 as suggested in [10] would not destabilize the cubic state. Here assuming negative J_1 and J_2 , we calculated eigenvalues of their Fourier transform $J(q)$ for the cubic state in the scheme of the LCAO (linear combination of atomic orbitals) approximation; see

Fig. 5(b). Further neighbor interactions are neglected for simplicity. A flat dispersion of $J(q)$ found along the highest P-(D)-N branch indicates macroscopic degeneracies of AF ground states [21]; the Mo sublattice is not fully frustrated like pyrochlore but is apparently frustrated for all AF states with $\mathbf{q} = (\frac{1}{2}\frac{1}{2}\xi)$ with arbitrary ξ . We also found that the suggested tetragonal deformation lifts the degeneracies. Thus we conclude that the cubic structure is unstable for negative J_2 . The lattice deformation may be spin-frustration-driven symmetry breakdown like the spin Jahn-Teller (JT) effect [2]. In Mo_3Sb_7 , the spin frustration triggers the tetragonal deformation to decouple the 3D isotropic AF interaction, and stabilizes spatial long-range order of spin-singlet dimers, i.e., the valence bond crystal. As the reduced χ from higher T ($\gg T_S$) and the considerably broadened specific heat (C) anomaly were reported [10], this state is realized instead of long-range AF order due to strong intra-dimer coupling already developed from sufficient high T .

Taking account of the motional narrowing of nuclear dipolar fields observed by μSR at $\sim T_S$, and structural characteristics of the low- T phase, we propose a scenario for the transition. First, note that the deformed states along [100], [010] and [001] directions are degenerate. Here we refer to the corresponding Mo electronic states as ψ_x , ψ_y and ψ_z . We expect that the high- T cubic state is the dynamic mixing of the three states, i.e., $(\psi_x + \psi_y + \psi_z)/3$, just like the vibronic dynamic JT state. In other words, harmonic oscillations of the valence bonds keeping strong intra-dimer interaction are thermally induced. The narrowing of $\mu\text{SR}-\Delta$, which reflects a relatively high-energy part of the dynamics, is explained naturally; at sufficiently low T , muons sense well defined nuclear dipolar fields from the deformed Mo

sublattice, which are averaged by the dynamic atomic motion with increasing T . NQR- $1/T_2$ above T_S , which nearly follows $\mu\text{SR}-\Delta$, is explained by the same mechanism, while the damping below T_S is ascribed to the decoupling of the nuclear spin-spin interaction, i.e., the reduction of Sb like-nuclei due to the separation of the Sb sites in the distorted state. It is of interest that magnetic entropy estimated from C exceeds $R \ln 2 \simeq 0.69R$ corresponding to the $S = 1/2$ manifold and is asymptotic to a much higher value $\sim 1.0R$ [10] close to $R \ln 3 \simeq 1.1R$ expected for the triply degenerate state.

In conclusion, NQR and μSR experiments revealed symmetry breakdown to a nonmagnetic state below $T_S \simeq 50$ K, with most probably tetragonal lattice distortion. Assuming negative J_1 and J_2 in the Mo sublattice, we pointed out possible frustration and proposed long-range order of spin-singlet dimers to the valence bond crystal, which transfers to the characteristic dynamic state with the cubic symmetry. Precise structural determination and experiments to detect phonon anomalies would be helpful to discuss the mechanism of the transition. On the other hand, NQR- $1/T_1$ demonstrated the s -wave SC emerged from a metallic state where high- T Mo spins are quenched. The electron itinerancy and the present description focusing on the local nature should be reconciled in further studies, similarly to in other geometrically frustrated metals [22].

We acknowledge T. Mito and K. Ueda for helpful discussions, Y. Narumi and K. Kindo at ISSP, the University of Tokyo, and Y. Tanaka at RIKEN, SPring-8 for collaboration. This work was supported by a grant from the University of Hyogo, and by Grant-in-Aid for Scientific Research on Priority Areas “Novel States of Matter Induced by Frustration” (19052003).

-
- [1] A. P. Ramirez, in *Handbook of Magnetic Materials*, edited by K. H. J. Buschow (North-Holland, Amsterdam, 2001).
 - [2] Y. Yamashita and K. Ueda, Phys. Rev. Lett. **85**, 4960 (2000).
 - [3] O. Tchernyshyov *et al.*, Phys. Rev. B **66**, 064403 (2002).
 - [4] M. Isobe and Y. Ueda, J. Phys. Soc. Jpn. **71**, 1848 (2002), M. Schmidt *et al.*, Phys. Rev. Lett. **92**, 056402 (2004), S. Di Matteo *et al.*, Phys. Rev. Lett. **93**, 077208 (2004).
 - [5] For example, R. Settai *et al.*, J. Phys. Soc. Jpn. **76**, 051003 (2007), H. Amitsuka *et al.*, Phys. Rev. Lett. **83**, 5114 (1999).
 - [6] Z. Bukowski *et al.*, Solid State Commun. **123**, 283 (2002).
 - [7] C. Candolfi *et al.*, Phys. Rev. Lett. **99**, 037006 (2007).
 - [8] U. Häussermann *et al.*, Chem. Eur. J. **4**, 1007 (1998), E. Dashjav *et al.*, J. Mater. Chem. **12**, 345 (2002).
 - [9] V. H. Tran *et al.*, arXiv: 0803.2948v1.
 - [10] V. H. Tran *et al.*, Phys. Rev. Lett. **100**, 137004 (2008).
 - [11] V. M. Dmitriev *et al.*, Supercond. Sci. Technol. **19**, 573 (2006).
 - [12] C. Candolfi *et al.*, Phys. Rev. B **77**, 092509 (2008).
 - [13] V. M. Dmitriev *et al.*, Low Temp. Phys. **33**, 295 (2007).
 - [14] J. D. Donaldson *et al.*, Acta Chem. Scand. A **28**, 866 (1974).
 - [15] D. E. MacLaughlin and J. D. Williamson, Phys. Rev. B **4**, 60 (1971).
 - [16] Below T_S , $1/T_1$ was measured at the peak position near 90 MHz, and the assumption of axial EFG is only for simplicity.
 - [17] Above T_S , $1/T_1$ varies roughly as $(T - T_S)^3$, suggesting unconventional electron-spin dynamics, presumably via electron-phonon coupling.
 - [18] L. C. Hebel and C. P. Slichter, Phys. Rev. **113**, 1504 (1959).
 - [19] Strictly speaking, the possibility of magnetic order cannot be excluded, when the internal field from Mo electrons is canceled at the muon site.
 - [20] In fact, the 600 reflection is superimposed with 442, of which intensity is smaller by one order.
 - [21] A. B. Harris *et al.*, Phys. Rev. B **45** (1992) 2899, J. N. Reimers *et al.*, Phys. Rev. B **43** (1991) 865.
 - [22] R. Ballou *et al.*, Phys. Rev. Lett. **76**, 2125 (1996), H. Nakamura *et al.*, J. Phys.: Condens. Matter **9**, 4701 (1997), S. Kondo *et al.*, Phys. Rev. Lett. **78**, 3729 (1997).